

AD-A088 674

OKLAHOMA UNIV NORMAN DEPT OF CHEMISTRY  
OXY AND THIO PHOSPHORUS ACID DERIVATIVES OF TIN. 4. DIORGANOTIN-- TC(U)  
AUG 80 J L LEFFERTS, K C MOLLOY  
N00014-77-C-0432  
NL

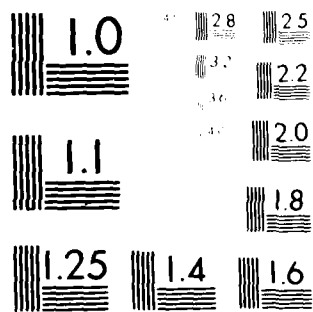
UNCLASSIFIED

1 OF 1

AD-A088 674

■

END  
DATE  
FILMED  
10-80  
DTIC



MICROCOPY RESOLUTION TEST CHART  
NATIONAL BUREAU OF STANDARDS-1963-A

AD A088674

DDC FILE COPY

SECURITY CLASSIFICATION OF THIS PAGE (When Data Entered)

## REPORT DOCUMENTATION PAGE

READ INSTRUCTIONS  
BEFORE COMPLETING FORM

1. REPORT NUMBER 18	2. GOVT ACCESSION NO. AD-A088674	3. RECIPIENT'S CATALOG NUMBER
4. TITLE (and Subtitle) Oxy and Thio Phosphorus Acid Derivatives of Tin. 4. Diorganotin(IV) Bis(dithiophosphate) Esters		5. TYPE OF REPORT & PERIOD COVERED
7. AUTHOR(s) J.L. Lefferts K.C. Molloy J. J. Zuckerman, I. Haiduc M. Curtui C. Guta and D. Ruse		6. PERFORMING ORG. REPORT NUMBER
9. PERFORMING ORGANIZATION NAME AND ADDRESS University of Oklahoma Department of Chemistry Norman, Oklahoma 73019		8. CONTRACT OR GRANT NUMBER(s) N00014-77-C-0432
11. CONTROLLING OFFICE NAME AND ADDRESS Office of Naval Research Department of the Navy Arlington, Virginia 22217		10. PROGRAM ELEMENT, PROJECT, TASK AREA & WORK UNIT NUMBERS NR 053-636
14. MONITORING AGENCY NAME & ADDRESS (if different from Controlling Office)		12. REPORT DATE 1 Aug 1980
		13. NUMBER OF PAGES
		15. SECURITY CLASS. (of this report) Unclassified
		15a. DECLASSIFICATION/DOWNGRADING SCHEDULE

## 16. DISTRIBUTION STATEMENT (of this Report)

Approved for Public Release, Distribution Unlimited

## 17. DISTRIBUTION STATEMENT (of the abstract entered in Block 20, if different from Report)

Prepared for Publication in Inorganic Chemistry

## 18. SUPPLEMENTARY NOTES

## 19. KEY WORDS (Continue on reverse side if necessary and identify by block number)

Organotins, Mössbauer Spectroscopy, Tin-119m Mössbauer Spectroscopy, Variable Temperature Mössbauer Spectroscopy, Lattice Dynamics, Diorganotins, Dithiophosphate Esters, Infrared Spectroscopy, Raman spectroscopy, Nuclear Magnetic Resonance Spectroscopy, Mass Spectroscopy, Effective Vibrating Mass Model, Phosphoric Acids, Dithiophosphate Esters, Synthesis, Condensation Reactions,

## 20. ABSTRACT (Continue on reverse side if necessary and identify by block number)

Eleven dimethyl- and diphenyltin bis(dithiophosphate)esters,  $R_2Sn[S_2P(OR')_2]_2$ , where  $R=CH_3$  and  $R'=CH_3, C_2H_5, n-C_3H_7$ , and  $i-C_3H_7$ , and where  $R=C_6H_5$  and  $R'=CH_3, C_2H_5, n-C_3H_7, i-C_3H_7, n-C_4H_9, i-C_4H_9$ , and  $C_6H_5$ , are synthesized in high yield by the reaction of the diorganotin dichlorides with the ammonium, sodium, or potassium salts of the dithiophosphoric ester or by the condensation of the diorganotin(IV) oxide with the O,O'-diorgano dithiophosphoric acid in benzene to release water which is distilled azeotropically to drive the reaction forward.

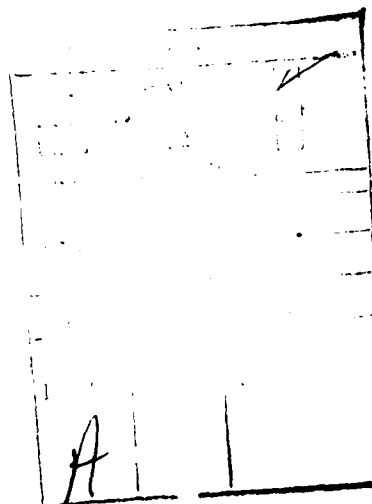
DD FORM 1 JAN 73 1473

EDITION OF 1 NOV 65 IS OBSOLETE  
S/N 0102-LF-014-6601Unclassified  
SECURITY CLASSIFICATION OF THIS PAGE (When Data Entered)

80 9 2 057

## 19. Esters.

20. The products are colorless, crystalline solids or oils, soluble in organic solvents. Infrared band assignments can be made in the case of the  $\nu(\text{CO})$  ( $1150\text{--}1145\text{ cm}^{-1}$ ),  $\nu(\text{POR})$  ( $1025\text{--}985\text{ cm}^{-1}$ ), and  $\nu(\text{PS}_2)$  ( $660\text{--}610\text{ cm}^{-1}$ ) modes, but the  $\nu_{\text{sym}}(\text{PS}_2)$  absorptions obscure the important (SnC) modes. NMR  $^2J$  ( $^{119}\text{Sn}\text{--}\text{C}\text{--}\text{H}$ ) coupling constants of 79–80 Hz for the methyltin derivatives are consistent with six-coordinated diorganotin species in solution, and mass spectral data are consistent with monomers. Tin-119m Mössbauer isomer shift (IS) values ( $1.35\text{--}1.47\text{ mm s}^{-1}$ ), [ratio of quadrupole splitting (QS) to IS] ( $2.18\text{--}2.65$ ), and QS values ( $3.12\text{--}3.67\text{ mm s}^{-1}$ ) specify diorganotin(IV) complexes in a six-coordinated, trans-octahedral geometry. Available C–Sn–C angle data for the ethyl ( $135^\circ$ ) and isopropyl ( $180^\circ$ ) ester derivatives allow the correlation with QS to be calibrated, and this relationship is used to predict the angles in the other diphenyltin systems studied. The ethyl and *n*-propyl ester derivatives behave roughly equivalently in a variable-temperature Mössbauer study, where the slope of the temperature dependence of the log of the resonance area is consistent with a structure consisting of noninteracting, monomeric molecules, and the two ester analogues are predicted to be approximately isostructural with a C–Sn–C angle of  $135^\circ$ . The isopropyl ester derivative is by contrast tightly packed into a strongly bound lattice in which short sulfur-sulfur atom contacts play an important role, and this is reflected in a much diminished slope.



# Experimental Section

Organotin starting materials were of commercial grade and were used without further purification. The dithiophosphoric acids and their sodium, potassium and ammonium salts were prepared by literature methods described in Part I of this series.<sup>1</sup> Carbon and hydrogen analyses were performed by Gailbraith Laboratories, Inc., Knoxville, Tennessee.

Infrared spectra were recorded on a Beckman 4250 spectrometer as Nujol mulls on KBr plates and polyethylene film. Mass spectra were recorded on a Hewlett-Packard 5985B mass spectrometer. Tin-119m Mössbauer spectra were recorded on a Ranger Engineering constant acceleration spectrometer equipped with an NaI scintillation counter and using  $\text{Ca}^{119\text{m}}\text{SnO}_3$  (New England Nuclear Corp.) as source and  $\text{Ca}^{119}\text{SnO}_3$  as standard reference material for zero velocity. Velocity calibration was based upon  $\beta$ -tin. Standard, non-linear, least-squares techniques were used to fit the data to Lorentzian curves. The Ranger Engineering variable temperature liquid nitrogen dewar and controller used in these studies is regulated by a variable-bridge, silicon-controlled-rectifier circuit, and is accurate to  $\pm 1\text{K}$ . Raman data were taken on a Spex Ramalog 5 laser Raman spectrometer.

The compounds studied are listed with the preparatory method used, their yields, melting points and microanalytical data in Table I. Tin-119m Mössbauer data are listed in Table II, and proton magnetic resonance, infrared and mass spectrometric data in Tables III, IV and V. Four typical preparations are described in detail below.

Bis-[0,0'-dimethyldithiophosphato]diphenyltin(IV),  $(\text{C}_6\text{H}_5)_2\text{Sn}[\text{S}_2\text{P}(\text{OCH}_3)_2]_2$ .

Diphenyltin dichloride (1.72 g, 0.005 mole) in diethylether (50 mL) was added to a solution of ammonium dimethyldithiophosphate (1.75 g, 0.01 mole) in anhydrous ethanol (110 mL), and the mixture was allowed to reflux for ca. 0.5h. The resulting precipitate was removed by filtration, and the

filtrate slowly concentrated to give the product as white crystals

(1.80 g, 62%), m.p. = 118°C.

Other similar compounds prepared by this method, with the amounts of reagents and yields, are tabulated below:

$R, R'$ in $R_2Sn[S_2P(OR')]_2$	$R_2SnCl_2$ g(moles)	$NH_4S_2P(OR')_2$ g(moles)	Yield g(%)
$CH_3, CH_3$	3.30 (0.015)	5.30 (0.03)	4.5 (70)
$CH_3, C_2H_5$	0.55 (0.0025)	1.01 (0.005)	1.0 (80)
$CH_3, n-C_3H_7$	3.30 (0.015)	6.93 (0.03)	7.0 (82)
$CH_3, i-C_3H_7$	2.20 (0.01)	4.70 (0.02) <sup>a</sup>	3.7 (65)
$C_6H_5, C_2H_5$	1.72 (0.005)	2.03 (0.01)	2.7 (82)
$C_6H_5, n-C_3H_7$	0.86 (0.0025)	1.17 (0.005)	1.2 (70)
$C_6H_5, i-C_3H_7$	1.72 (0.005)	2.31 (0.01)	3.1 (88)
$C_6H_5, n-C_4H_9$	0.86 (0.0025)	1.30 (0.005)	0.6 (33)

<sup>a</sup> in water (50 mL).

Bis-[0,0'-dimethyldithiophosphato]dimethyltin(IV),  $(CH_3)_2Sn[S_2P(OCH_3)_2]_2$ .

Metallic sodium (0.46g, 0.02 mole) was dissolved in absolute ethanol (50 mL) and the resulting solution treated with dimethyldithiophosphoric acid (3.16g, 0.02 mole). A solution of dimethyltin dichloride (2.20 g, 0.02 mole) in absolute methanol was added to form a white precipitate of NaCl which was separated by filtration. The filtrate was concentrated to give a white crystalline product (3.15 g, 68%), m.p. = 82°C.

Other compounds prepared by this method are listed below:

$R'$ in $(CH_3)_2Sn[S_2P(OR')]_2$	$(CH_3)_2SnCl_2$ g(moles)	$HS_2P(OR')_2$ g(mole)	Yield g(%)
$C_2H_5$	2.20 (0.01)	3.72 (0.02)	3.70 (71)
$n-C_3H_7$	2.20 (0.01)	4.28 (0.02)	3.45 (60)
$i-C_3H_7$	2.20 (0.01)	4.28 (0.02)	2.20 (40)

Bis-[0,0'-diphenyldithiophosphato]diphenyltin(IV),  $(C_6H_5)_2Sn[S_2P(OC_6H_5)_2]_2$ .

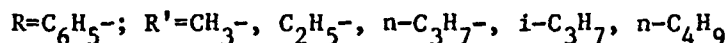
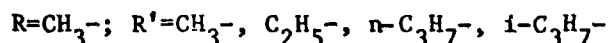
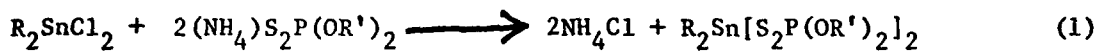
A suspension of diphenyltin(IV) oxide (2.89, 0.01 mole) and diphenyldithiophosphoric acid (5.64 g, 0.02 moles) in benzene (100 mL) was allowed to reflux for ca. 1 h, and the water formed in the reaction separated azeotropically by a Dean and Stark apparatus. The cooled solution was filtered to remove trace amounts of solid and concentrated to ca. 10 mL. The solid that precipitated was redissolved in hot toluene, crystallized at 0°C, filtered and washed with hexane to yield a cream-colored solid. Recrystallization from n-hexane/toluene (3:1) yielded 5.82g (70%) of pure product, m.p. 145.5-146.5°C.

Bis-[0,0'-diisobutyldithiophosphato]diphenyltin(IV),  $(C_6H_5)_2Sn[S_2P(O-i-C_4H_9)_2]_2$ .

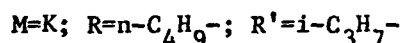
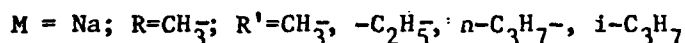
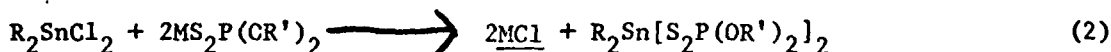
Diphenyltin(IV) oxide (2.89 g, 0.01 mole) and diisobutyldithiophosphoric acid (4.84 g, 0.02 mole) were refluxed together in benzene (100 mL) for 12 h, as outlined above. Concentration of the resulting solution afforded a colorless oil, which was recrystallized from hexane at -78°C to give the crude product as a white solid. Subsequent recrystallization from n-hexane at 0°C produced 5.02 g (66%) of a pure, white crystalline product, m.p. 82.5-83°C.

# Results and Discussion

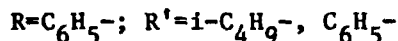
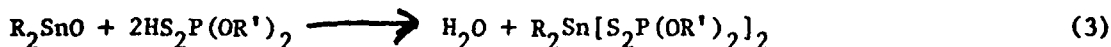
The diorganotin(IV) bis-(dithiophosphate) esters can be synthesized in high yield by the action of the ammonium salt of the appropriate acid ester upon the diorganotin(IV) dichloride in an ether-ethanol solvent mixture:



or by the use of an alkali metal salt of the acid ester and ethanol as the solvent:



or by the action of the acid esters themselves upon the diorganotin(IV) oxide in benzene:



The released water is distilled azeotropically to drive the reaction forward.

Syntheses (1) and (2) have been previously used to prepare the  $R=n-C_4H_9-$ ;

$R'=C_2H_5-$ -derivative, the latter from the sodium salt.<sup>7</sup> The  $R=n-C_4H_9-$

$R'$ =methylcyclohexyl- and octylphenyl- and  $R$ =didodecyl-;  $R'=i-C_3H_7-$  deri-

vatives have been prepared by synthesis (2) using the potassium salt,<sup>8,9</sup>

and the  $R=n-C_4H_9-$ ;  $R'$ =2-ethylhexyl- derivatives have been prepared by

synthesis (3).<sup>10</sup>



The organotin dithiophosphate esters in Table I are air stable, colorless, crystalline solids, soluble in polar and non-polar organic solvents.

In principle the possible structures for this series of compounds include a four-coordinated,  $R_2Sn[\overset{S}{\underset{S}{P}}(OR')_2]_2$  configuration containing monodentate dithiophosphate ester groups, but unchelated dithiophosphate systems are rare.<sup>11</sup> Why both the adduct  $Ni[S_2P(OCH_3)_2]_2 \cdot 2,9\text{-dimethyl-1,10-phenanthroline}$ <sup>12</sup> and  $0,0'\text{-diethyldithiophosphatotriphenyltin(IV)}$ ,  $(C_6H_5)_3SnS_2P(OC_2H_5)_2$ , whose structure we have recently solved as part of this series of investigations,<sup>2</sup> should contain monodentate dithiophosphate ester groups is not known. It is of interest that the closely related parent 1,10-phenanthroline complex of the former<sup>12</sup> and other corresponding trimethyltin(IV) derivatives of the latter<sup>1</sup> contain chelating groups. The bidentate dithiophosphate ester ligands can either be bridging or chelating, and an ionic form,  $[R_2Sn]^{2+}[S_2P(OR')_2]_2^{2-}$ , is also possible.

In the case of two of the derivatives, however, the crystal structures are known. Bis-[0,0'-diethyldithiophosphato]diphenyltin(IV) is octahedral with chelating, anisobidentate dithiophosphate ester ligands in which the two sets of tin-sulfur distances are 2.5 and 3.2 Å (the four sulfur atoms are located in the equatorial plane), and the diphenyltin system makes a C-Sn-C angle of 135°. The corresponding isopropyl ester derivative, bis-[0,0'-diisopropyldithiophosphato]diphenyltin(IV),  $(C_6H_5)_2Sn[S_2P(OR_{3H_7-i})_2]_2$ , adopts a trans-octahedral configuration which is, on the other hand, extremely symmetrical with tin-sulfur distances of 2.7 Å and an angle of 180° in the diphenyltin system. These molecules are packed very tightly into their lattice, such that a conversion to a bridged polymeric form could be accomplished with no further movement of the monomeric units closer together.<sup>4</sup>

In all likelihood then, the series of compounds synthesized here will adopt trans-octahedral geometries with bidentate, chelating dithiophosphate ester groups as is generally found in other derivatives of the main group and transition elements.<sup>10</sup>

Infrared Spectra. Infrared data cannot in any case distinguish the various structural possibilities, since it is impossible to assign with confidence the P-S and P=S stretching frequencies. For example, bands probably associated with the P-S stretching frequencies in the transition metal complexes which contain bidentate, chelating dithiophosphate ester ligands appear in the same region as for the free acids,  $(RO)_2\overset{\overset{S}{\parallel}}{P}SH$  and their esters,  $(RO)_2\overset{\overset{S}{\parallel}}{P}SR'$ .<sup>14</sup> There seems little sensitivity on the part of the observed frequencies at 560-530 and 670-630  $cm^{-1}$ ,<sup>15</sup> probably corresponding to  $\nu_{sym}(PS_2)$  and  $\nu_{asym}(PS_2)$ , respectively, to the nature of the groups connected to sulfur.<sup>15,16</sup>

The infrared data for our compounds are listed in Table IV. The  $\nu_{sym}(PS_2)$  absorptions obscure the important  $\nu(Sn-C)$  frequencies, which could yield information concerning the configuration of the C-Sn-C skeletons. While frequencies in the  $\nu(CO)$  region are observed in the 1170-1145  $cm^{-1}$  range, in the  $\nu(POR)$  region in the 1025-985  $cm^{-1}$  range,<sup>17</sup> and in the  $\nu(PS_2)$  region in the 660-610  $cm^{-1}$  range for the compounds listed, none of the assignments can be made with confidence because of the richness of the spectra. The  $PS_2$  modes have been assigned in the analogous organolead,<sup>18</sup> thallium<sup>16</sup> and mercury<sup>19</sup> derivatives.

Nmr Spectra. Chemical shifts and NMR coupling constant data are listed in Table III. Resonances which can be assigned to the phenyltin protons fall in the range 8.27 to 7.32 ppm; in bis-[0,0'-diphenyldithiophosphato]diphenyltin(IV),  $(C_6H_5)_2Sn[S_2P(OC_6H_5)_2]_2$ , the thirty  $C_6H_5Sn$  and  $OC_6H_5$  protons fall in the range 7.83-6.80 ppm. The expected integrated areas and peak multiplicities for the organic ester groups attached to

phosphorus through oxygen are observed in the spectra as indicated in the table. For example in the spectrum of bis-[0,0'-dimethyldithiophosphato] diphenyltin(IV),  $(C_6H_5)_2Sn[S_2P(OCH_3)_2]_2$ , the methoxy group signal appears as a doublet arising from the coupling  $|^3J(^{31}P-O-C-^1H)|=15.5\text{Hz}$ , and in the corresponding ethoxy derivative the methylene protons appear as a doublet of quartets arising from a coupling of 10.0 Hz to the phosphorus-31 nucleus, and the coupling  $|^3J(^1H-C-C-^1H)|=7.0\text{ Hz}$  with the terminal methyl protons of the ethyl group. The methyltin couplings  $|^2J(^{119}Sn-C-^1H)| = 80.0$  and 79.0 Hz, respectively, for the methoxy- and ethoxy esters, in the range expected for six-coordinated, diorganotin species in the dilute solutions in which they were recorded.<sup>20</sup>

Mass Spectra. The typical mass spectral data of the dimethyl- and diphenyltin dithiophosphate esters listed in Table V are quite similar. In none of the spectra are there any fragments of higher mass than the monomer, nor is there a parent molecular ion detectable, nor any arising from polytin species, thus ruling out any gas phase association of these monomers. The most abundant tin-bearing ion arises in each case from the loss of one of the dithiophosphate ester ligands. The successive loss of the organic groups from the tin atom is also a feature of these spectra. In addition there is the loss of alkene from the ester portion of all the dithiophosphate ligands except where  $R' = CH_3-$  and  $C_6H_5-$ .

A reasonable pathway for the decomposition of these esters appears to be by sequential loss of alkene from those dithiophosphate groups where this is possible, after initial loss of one ligand molecule and the organic group from tin. Thus for the dimethyltin ethyl ester, prominent fragments arise at  $m/e = 505[P-CH_3]^+$  and  $490[P-2CH_3]^+$  owing to the successive loss of methyl groups,  $m/e = 335[P-S_2P(OC_2H_5)_2]^+$  and  $150[P-S_2P(OC_2H_5)_2]^+$  owing to the successive loss of ligand molecules, and  $m/e = 307[P-L-C_2H_4]^+$  and  $279[P-L-2C_2H_4]^+$  owing to the

successive loss of ethylene. As in the case of the trimethyltin derivatives<sup>1</sup>, most of the high abundance fragments are even electron ions (see, for example, Table V).

Mössbauer Spectra. The tin-119m Mössbauer data listed in Table II can be interpreted in terms of diorganotin(IV) complexes in a six-coordinated, trans-octahedral configuration. The magnitudes of the Isomer Shift (I.S.) values (1.35 to 1.47 mms<sup>-1</sup>) specify a tin(IV) oxidation state. The magnitudes of the  $\rho$ -values [ratio of Quadrupole Splitting (Q.S.) to I.S.] (2.18 to 2.62) reflect a higher than four-coordinated situation at the tin atom, while the magnitudes of the Q.S. values (3.12 to 3.67 mms<sup>-1</sup>) are indicative of a trans-diorganotin configuration in an octahedral geometry.<sup>21</sup>

The variation in the magnitude of the Q.S. with the angle C-Sn-C for six-coordinated diorganotin compounds has been calculated from a point charge approach<sup>22</sup> given by:

$$|Q.S.| = 4\{R\}[1-3\sin^2\theta\cos^2\theta]^{1/2} \quad (1)$$

where  $\{R\}$  = partially quadrupole splitting for group R ( $-0.95\text{mms}^{-1}$  for  $R=\text{C}_6\text{H}_5$ <sup>23</sup>) and C-Sn-C =  $(180-2\theta)^\circ$ . The treatment assumes that there will be no sign inversion in the Q.S. data throughout the systems compared, that the partial Q.S. values for the ligands are small compared to that for the phenyl ligand, and that  $\{C_6H_5\}$  is a constant over the compounds studied. Nevertheless, this correlation is supported by the abundant structural data for six-coordinated dimethyltin(IV) compounds<sup>22</sup>, although for the corresponding diphenyltin(IV) system surprisingly few crystal structure studies are available.<sup>24</sup> The data for the compounds for which both Mössbauer and phenyl-tin-phenyl C-Sn-C angles are available are plotted in Figure 1, and listed in Table VI along with the predicted C-Sn-C angles given by the correlation expressed in Eq. 1 above, for the remaining diphenyltin dithiophosphates whose Q.S. values are known.

Variable-Temperature Mössbauer Study. Three compounds have been subjected to variable-temperature Mössbauer study, and the results are depicted in Figure 2. The Mössbauer recoil-free fraction,  $f$ , is related to the mean-square-displacement,  $\langle x^2 \rangle$ , of the tin atom from its equilibrium position:

$$f = \exp\left[-\frac{\langle x^2 \rangle}{\lambda^2}\right] \quad (2)$$

where  $\lambda$  is the wavelength of the Mössbauer gamma-ray divided by  $2\pi$ . For thin absorbers, using the Debye model,  $f$  is linearly related to the area under the Mössbauer resonance,  $A_T$ , and its temperature dependence is given by:

$$A_T \propto f = \exp\left[-\frac{6E_R T}{K\theta_D^2}\right] \text{ for } T \geq \frac{\theta_D}{2}$$

where  $E_R$  is the Mössbauer recoil energy and  $\theta_D$  is the Debye temperature of the solid. Thus, in the high temperature limit, plots of  $A_T$  vs. temperature should be linear. It is found that the more tightly bound the tin atoms are in a lattice, the slower will be the fall in  $f$ , and hence  $A_T$ , as the temperature is raised. Compounds of known structure containing non-interacting, monomeric molecules exhibit slopes of ca.  $-1.8 \times 10^{-2} \text{K}^{-1}$ , no matter what the coordination number at tin. Weak intermolecular interactions such as hydrogen bonding reduce this value to ca.  $-1.7 \times 10^{-2} \text{K}^{-1}$ , while a more complex system of hydrogen bonds can reduce it further to ca.  $-1.3 \times 10^{-2} \text{K}^{-1}$ . Strongly hydrogen bonded lattices and solids in which one-, two- and three- dimensional association is present exhibit slopes of ca.  $-0.9 \times 10^{-2} \text{K}^{-1}$ . The lowest value,  $-0.23 \times 10^{-2} \text{K}^{-1}$ , is given by tin(II) oxide.<sup>25-28</sup>

According to these systematics, the magnitudes of the slopes of the plots of  $\ln A_T$  vs. temperature for the ethyl- ( $-1.92 \times 10^{-2} \text{K}^{-1}$ ) and n-propyl ( $-2.19 \times 10^{-2} \text{K}^{-1}$ ) esters correspond to an arrangement of non-interacting monomeric molecules in the solid. The X-ray crystal structure of the ethyl derivative which is a badly distorted octahedral complex of tin is corroboratory, and it is likely from the

magnitudes of both the slope in Figure 2 and the Q.S. (3.12 vs. 3.22  $\text{mms}^{-1}$ ) that the n-propyl analogue is roughly isostructural in being a six-coordinated, distorted octahedron with a C-Sn-C angle essentially the same ( $135^\circ$ ) as found in the ethyl derivative (vide supra). Comparison can be drawn with the corresponding slope data for tetraphenyltin(IV),  $-1.659 \times 10^{-2} \text{K}^{-1}$  <sup>29,30</sup>, for which a Mössbauer spectrum at room temperature can be resolved. <sup>31</sup>

The isopropyl ester derivative,  $(\text{C}_6\text{H}_5)_2\text{Sn}[\text{S}_2\text{POC}_3\text{H}_7\text{-i})_2]_2$ , stands as an exception to the systematics thus far developed in correlating the slope data vs. structure. The magnitude of  $-1.06 \times 10^{-2} \text{K}^{-1}$  may be interpreted in terms of an associated solid into which tin atoms are bound in a one-, two- or three- dimensional polymeric lattice. Instead, the X-ray crystal structure reveals an arrangement of symmetrical, octahedral monomers in which there are very short sulfur-sulfur atom contact distances which define an axis of propagation through the crystal. The tin-tin atom distances along this axis ( $6.34\text{\AA}$ ) are such that pairs of metal atoms could be bridged by the dithiophosphate ligands without significantly altering the bite distance between the sulfur atoms. Thus the ligands could be shifted along the axis from a chelating position to a bridging position with no change in internuclear distances, or for that matter in the density of the resulting solid. We have termed this situation a "virtual polymer."<sup>4</sup> Care must, therefore, be exercised in interpreting this type of slope information in terms of molecular structure.

The Effective Vibrating Mass Model. This treatment combines data from the variation of the recoil-free fraction with temperature with the low energy ( $<200 \text{ cm}^{-1}$ ) lattice mode absorptions in the Raman spectrum to yield the mass of the vibrating unit in the solid. <sup>32</sup> The molecularity of the vibrating unit is calculated from:

$$M_{\text{eff}} = - \frac{3E_p^2 k}{(hc)^2 \omega_L^2} \left( \frac{dT}{d \ln A} \right) \quad (3)$$

where  $\frac{d\ln A}{dT}$  is the slope of the plot of the normalized area under the Mössbauer resonance vs. temperature for which data for three compounds have been discussed above, and  $E_\gamma$  is the energy (23.8 KeV) of the Mössbauer gamma-ray. The low energy Raman spectra which should contain the frequency  $\omega$ , are shown in Figure 3 for the ethyl- and isopropyl ester derivatives.

The spectrum of the n-propyl derivatives lacks bands which could be reasonably assigned to this mode. This has been noted in the case of  $[\text{Sn}(\text{SCH}_2\text{CH}_2\text{S})_2]_n$  where the mode sought is only observable at low temperature (77K).<sup>31</sup> The molecular weights of the ethyl- and isopropyl monomers are 643.37 and 699.49, respectively. Thus no band in either spectrum above those found at 28 and 34  $\text{cm}^{-1}$ , respectively, can correspond to the unique, intermolecular, intra-unit cell vibration sought in this treatment. The 28  $\text{cm}^{-1}$  band in the spectrum of the ethyl ester derivative corresponds closely, as can be seen from the data displayed in Table VI, to the monomer, but the 34  $\text{cm}^{-1}$  band for the isopropyl analogue is in only moderate agreement with its corresponding monomer value. In this latter case the bands at 25 and 16  $\text{cm}^{-1}$  must also be considered, and a polymeric structure cannot be ruled out. The X-ray crystal structure information discussed above is corroboratory, and the description in terms of a "virtual-polymer" is thus not unreasonable.<sup>4</sup>

Temperature Variation of the Goldanskii-Karyagin Effect. The anisotropy of the Mössbauer recoil-free fraction, commonly called the Goldanskii-Karyagin effect<sup>33,34</sup> and observed as an asymmetry of the relative intensities of the two lines of a doublet spectrum, can also yield information concerning the lattice dynamics of solids, especially if X-ray diffraction data are also available. In our case the structures of both the ethyl and isopropyl derivatives are available, and the trans- C-Sn-C axis can be defined as the z-axis by analogy with the published treatment of  $(\text{CH}_3)_2\text{Sn}(\text{C}_5\text{H}_7\text{O}_2)_2$ ,<sup>35</sup> whose structure is also known.<sup>36</sup> For  $(\text{C}_6\text{H}_5)_2\text{Sn}[\text{S}_2\text{P}(\text{OC}_2\text{H}_5)_2]_2$ , the z-axis is defined as the idealized C-Sn-C axis in which this vector is linear. The motion perpendicular to the axis for both esters lies in the plane of the two chelating ligands. In cases such as this

it is possible to derive from the Mössbauer data two separate effective Debye temperatures corresponding to the motion of the tin atom parallel and perpendicular to this axis. The combined effect of the anisotropies in the electric charge density and the force constants results in the temperature-dependent asymmetry of the Mössbauer doublet. The ratio of the areas of the two wings of the doublet can then be related to the mean square vibrational amplitudes parallel and perpendicular to the symmetry axis if the shape of the electric charge distribution about the tin atom is known. From previous X-ray<sup>24</sup> and Mössbauer<sup>35</sup> studies it is known that the motion of the tin atom is more constrained in the equatorial plane of octahedral, trans-diorganotin complexes than along the C-Sn-C bonds, and in the two compounds for which structural data are available the two components of the Mössbauer resonance doublet are easily resolved and the areas measured (Tables VIII, IX), and large resonance effects are observed even for thin absorbers. It is possible to obtain information about the mean-square amplitudes of vibration parallel ( $\langle x_{\parallel}^2 \rangle$ ) and perpendicular ( $\langle x_{\perp}^2 \rangle$ ) to the z-axis by measuring the temperature dependence of the areas of the two resonance lines. Plots of the temperature dependence of  $\langle x_{\parallel}^2 \rangle$  and  $\langle x_{\perp}^2 \rangle$  for the ethyl and isopropyl ester derivatives are shown in Figures 5 and 6, respectively. The description of the treatment follows.

As in the case of dimethyltin(IV) bis-acetylacetonate<sup>35</sup> we assume a prolate shape for the electrostatic field about the z-axis of cylindrical symmetry (C-Sn-C), and hence that  $V_{zz}$ , the principle component of the electric field gradient tensor, is negative. a prolate field acting on a tin-119m nucleus moves the spin 3/2 level to higher energy with respect to the spin 1/2 level, and R (the ratio of the area under the more positive velocity component of the quadrupole doublet to the area of the more negative component) =  $A_+/A_- = A_{\pi}/A_0$ . Consequently, the doublet component a higher velocities corresponds to the  $\Delta m = +1(\pi)$  transition and the lower one



to the  $\Delta m = 0$  ( $\sigma$ ) transition. In the trans-diorganotin octahedra studied here, the bulk of the electron density would be expected to lie along the C-Sn-C axis, and hence a prolate field and negative  $V_{zz}$  are reasonable.

The mean square amplitudes of vibration parallel and perpendicular to  $V_{zz}$  can be expressed as:

$$A \{ \ln f = - \frac{1}{3\kappa^2} [2\langle x_{\parallel}^2 \rangle + \langle x_{\perp}^2 \rangle] \quad (4)$$

or in terms of an asymmetry factor,  $\epsilon$ , where:

$$\epsilon = [\langle x_{\parallel}^2 \rangle - \langle x_{\perp}^2 \rangle] / \kappa^2 \quad (5)$$

and hence:

$$\langle x_{\parallel}^2 \rangle = \kappa^2 \left( \frac{2\epsilon}{3} - \ln f \right) \quad (6)$$

$$\text{and } \langle x_{\perp}^2 \rangle = -\kappa^2 \left( \frac{\epsilon}{3} + \ln f \right) \quad (7)$$

Of the four variables in these two equations,  $\epsilon$ ,  $f$ ,  $\langle x_{\parallel}^2 \rangle$  and  $\langle x_{\perp}^2 \rangle$ ,  $\epsilon$  can be calculated from the temperature dependence of  $A_{\pi}/A_{\sigma}$ , and  $f$  from the temperature dependence of the total area under the resonance plus one value of  $f$ . This latter value may be derived indirectly from the X-ray thermal data at the temperatures at which the crystal structures were determined (298K for the ethyl ester and 138K for the isopropyl ester derivative) using Equation (2).

The temperature dependence of the total area is used to generate the data used to construct Figures 5 and 6. It is seen that since  $R < 0$  the asymmetry parameter,  $\epsilon$ , is always positive, that is,  $\langle x_{\parallel}^2 \rangle > \langle x_{\perp}^2 \rangle$  in the temperature range measured.<sup>37</sup> The equations of the two plots for the ethyl ester are:

$$\langle x_{\parallel}^2 \rangle = 2.21 \times 10^{-4} T + 7.13 \times 10^{-3} \quad (8)$$

(correlation coefficient 0.969, number of points 7, in the temperature range 77 to 135K), and

$$\langle x_{\perp}^2 \rangle = 8.66 \times 10^{-5} T + 1.12 \times 10^{-2} \quad (9)$$

(correlation coefficient 0.951, number of points 7, in the temperature range 77 to 135K). The corresponding plots for the isopropyl ester are:

$$\langle x_{\parallel}^2 \rangle = 1.28 \times 10^{-4} T + 2.56 \times 10^{-4} \quad (10)$$

(correlation coefficient 0.811, number of points 8, in the temperature range 77 to 145K), and

$$\langle x_{\perp}^2 \rangle = 4.17 \times 10^{-5} T + 2.47 \times 10^{-3} \quad (11)$$

(correlation coefficient 0.730, number of points, 8, in the temperature range 77 to 145K). The mean square amplitudes of vibration from the Mössbauer experiment for the ethyl ester are  $1.80 \times 10^{-2}$  and  $2.42 \times 10^{-2}$  for  $\langle x^2 \rangle$  and  $\langle x_{\parallel}^2 \rangle$ , respectively, at 77K and  $2.35 \times 10^{-2}$  and  $3.60 \times 10^{-2}$  at 135K. The corresponding data for the isopropyl analogue are  $0.65 \times 10^{-2}$  and  $0.81 \times 10^{-2}$  at 77K and  $0.68 \times 10^{-2}$  and  $1.94 \times 10^{-2}$  at 135K for direct comparison.

From these observations we can see that while both the  $-S_2P(OR)_2$  ligands chelate their respective tin atoms, the  $R' =$  isopropyl ester ligand does so more tightly, giving rise to  $\langle x_{\perp}(T)^2 \rangle_{C_2H_5} > \langle x_{\perp}(T)^2 \rangle_{C_3H_7-i}$  for all T values measured, and also  $\frac{d\langle x_{\perp}(T)^2 \rangle_{C_2H_5}}{dT} > \frac{d\langle x_{\perp}(T)^2 \rangle_{C_3H_7-i}}{dT}$ . The "virtual polymer" nature of the  $R = i-C_3H_7$  lattice which propagates along a plane containing the  $Sn[S_2P(OC_3H_7-i)]_2$  units also contributes to this effect.

In addition, while for  $R' = i-C_3H_7$  the angle C-Sn-C is  $180^\circ$  so that the bulky phenyl group lies along the z-axis, for the  $R' = C_2H_5$  structure

these atoms make an angle of only  $135^\circ$  and hence do not lie completely along the axis. This fact helps to explain why  $\langle x_{||}(T)^2 \rangle_{C_2H_5} \gg \langle x_{||}(T)^2 \rangle_{C_3H_7-i}$

$$\text{and } \frac{d\langle x_{||}(T)^2 \rangle_{C_2H_5}}{dT} > \frac{d\langle x_{||}(T)^2 \rangle_{C_3H_7-i}}{dT}.$$

Both factors contribute to the difference in the slopes of the area under the Mössbauer resonance vs. temperature which are  $-1.06 \times 10^{-2} K^{-1}$  for  $R = C_3H_7-i$  and  $-1.92 \times 10^{-2} K^{-1}$  for  $R' = C_2H_5$ .

The calculation of absolute values of mean-square amplitudes of vibration is based upon knowledge of one value of  $f$ , which is in this treatment derived from a known value of  $\langle x^2 \rangle$  obtained from the X-ray data. Since this latter parameter in the X-ray experiment has inherent and undeterminable errors, the calculated values of  $\langle x_L^2 \rangle$  and  $\langle x_{||}^2 \rangle$  will propagate this error, and are thus quoted only as a guide to the relative changes in the directional amplitudes of motion of the Mössbauer atom. However, the temperature coefficients of these vibrations (i.e., the slopes of the lines in Figures 5 and 6) are independent in this treatment of an absolute value of  $f$ , and hence the need for  $\langle x^2 \rangle$  from the X-ray data. The coefficients are characteristic of the two samples studied, and enable comparison of the chelating power of the dithio-phosphate ligands. This treatment is capable of extension to other chelating systems, where it can serve to measure the relative binding powers of the ligands without having X-ray data available.

Acknowledgements.

Our work is supported by the Office of Naval Research and by the National Science Foundation through Grant CHE-78-26584. We thank M&T Chemicals, Inc. for the donations of organotin starting materials, and Professor R.E. Frech of the University of Oklahoma for help with the Raman spectra

References and Notes

- (1) Lefferts, J.L.; Molloy, K.C.; Zuckerman, J.J.; Haiduc, I.; Guta, C; Ruse, Inorg. Chem., 1980, 19, in press.
- (2) Molloy, D.C.; Hossain, M.B.; van der Helm, D.; Zuckerman; J.J.; Inorg. Chem. 1979, 18, 3507.
- (3) Hossain, M.B.; Lefferts, J.L.; Molloy, K.C.; van der Helm, D.; Zuckerman, J.J.; submitted for publication.
- (4) Molloy, K.C.; Hossain, M.B.; van der Helm, D.; Zuckerman, J.J.; Haiduc, I.; Inorg. Chem., 1980, 19, in press.
- (5) Zuckerman, J.J., editor, Organotin Compounds: New Chemistry and Applications, Advances in Chemistry Series, No. 157, American Chemical Society, Washington, DC, 1976.
- (6) Zuckerman, J.J.; Reisdorf, R.P.; Ellis, H.V., III; Wilkinson, R.R., Chemical Problems in the Environment: Occurrence and Fate of the Organoelements, ed. by Bellama, J.M.; Brinkman, F.E. ACS Symposium Series No. 82. American Chemical Society, Washington, DC, 1978, 388.
- (7) Lapitskii, G.A.; Granenkina, L.S.; Khokhlov, P.S.; Bliznyuk, N.K.; J. Gen. Chem. USSR, 1968, 38, 2689.
- (8) Esso Research and Engineering Co., U.S. Pat. 2,786,812 (1957); Chem. Abstr. 1957, 51, 10892f.
- (9) Esso Research and Engineering Co., Brit. Pat. 737,392 (1955); Chem. Abstr. 1956, 50, 9010
- (10) Yoshitomi Pharmaceutical Industries, Jap. Pat. 15,290 (1966); Chem. Abstr. 1966, 65, 20164f.
- (11) Wasson, J.R.; Woltermann, G.M.; Stoklosa, H.J. Forsch. Chem. Forsch. 1973, 35, 65.
- (12) Shetty, P.S.; Fernando, Q. J. Am. Chem. Soc. 1970, 92, 3964.
- (13) Liebllich, B.W.; Tomassini, M. Acta Crystallogr., Sect. B 1978, 34, 944.
- (14) Chittenden, R.A.; Thomas, L.C. Spectrochim. Acta 1964, 20, 1679.
- (15) Adams, D.M.; Cornell, J.B. J. Chem. Soc., A 1968, 1299.
- (16) Walther, B. Z. Anorg. Chem. 1972, 395, 211.
- (17) Walther, B. Z. Anorg. Chem. 1972, 395, 211.
- (18) Haiduc, I.; Martinas, F.; Ruse, D.; Curtui, M. Syn. React. Inorg. Metal. Org. Chem. 1975, 5, 103.
- (19) Haiduc, I.; Veres, E. Syn. React. Inorg. Metal.-org. Chem. 1975, 5, 115.
- (20) Petrosyan, V.S. Prog. NMR Spectrosc. 1977, 11, 115.
- (21) Zuckerman, J.J. Advan. Organometal. Chem. 1970, 9, 21.
- (22) Sham, T.K.; Bancroft, G.M. Inorg. Chem. 1975, 14, 2281.

- (23) Clark, M.G.; Maddock, A.G.; Platt, R.H. J. Chem. Soc., Dalton Trans. 1972, 210.
- (24) Zubieta, J.A.; Zuckerman, J.J. Prog. Inorg. Chem. 1978, 24, 251
- (25) Harrison, P.G.; Phillips, R.C.; Thornton, E.W. J. Chem. Soc., Chem. Commun. 1977, 603.
- (26) Harrison, P.G.; Molloy, K.C.; Thornton, E.W. Inorg. Chim. Acta 1978, 33, 137.
- (27) Harrison, P.G.; Begley, M.J.; Molloy, K.C. J. Organomet. Chem. 1980, 186, 213.
- (28) Herber, R.H.; Leahy, M.F. J. Chem. Phys. 1977, 67, 2718.
- (29) Reported as  $-1.60 \times 10^{-2} \text{K}^{-1}$  in ref 30.
- (30) Hazony, Y.; Herber, R.H. in Mössbauer Effect Methodology, ed. by Gruverman, I.; Seidel, C.W. Plenum Press, New York, Vol. 8, 1978, p. 107.
- (31) Bancroft, G.M.; Butler, K.D.; Sham, T.K. J. Chem. Soc., Dalton Trans. 1975, 1483.
- (32) Herber, R.H.; Leahy, M.F. in Organotin Compounds: New Chemistry and Applications, ed. by Zuckerman, J.J., ACS Advances in Chemistry Series, No. 157, American Chemical Society, Washington, D.C., 1976, p. 155.
- (33) Greenwood, N.N.; Gibb, T.C. Mössbauer Spectroscopy, Chapman and Hall, London, 1971.
- (34) Gibb, T.C. Principles of Mössbauer Spectroscopy, Chapman and Hall, London, 1976.
- (35) Herber, R.H.; Leahy, M.F.; Hazony, Y. J. Chem. Phys. 1974, 60, 5070.
- (36) Miller, G.A.; Schlemper, E.O. Inorg. Chem. 1973, 12, 677.
- (37) Flinn, P.; Ruby, S.L.; Kehl, W.L. Science, 1964, 143, 1434.
- (38) Poller, R.C.; Ruddick, J.N.R.; Taylor, B.; Toley, D.L.B. J. Organometal. Chem., 1970, 24, 341.
- (39) Coghi, L.; Nardelli, M.; Pelizzi, C.; Pelizzi, G. Gazz. Chim. Ital., 1975, 105, 1187.
- (40) Liengme, B.V.; Randall, R.S.; Sams, J.R. Canad. J. Chem., 1972, 50, 3212.
- (41) Parish, R.V.; Platt, R.H. Inorg. Chim. Acta., 1970, 4, 65.
- (42) Harrison, P.G.; King, T.J.; Richards, J.A. J. Chem. Soc. Dalton. Trans., 1976, 2317.
- (43) Thompson, D.W.; Barrett, P.B.; Lefelhocz, J.F.; Lock, G.A. J. Coord. Chem., 1973, 3, 119.
- (44) Lindley, P.F.; Carr, P. J. Cryst. Mol. Struct., 1974, 4, 173.

Table I. Diorganotin(IV) Bis-[dithiophosphate] Esters

<u>R</u>	<u>R'</u>	<u>Preparation</u>	<u>Yield (%)</u>	<u>m.p. (°c)</u>	<u>%P</u>	
					<u>Calc.</u>	<u>Found</u>
CH <sub>3</sub>	CH <sub>3</sub>	1,2	50,68	82	13.40	12.80
CH <sub>3</sub>	C <sub>2</sub> H <sub>5</sub>	1,2	80,71	32-33	11.90	11.10
CH <sub>3</sub>	n-C <sub>3</sub> H <sub>7</sub>	1,2	82,60	oil	10.80	9.80
CH <sub>3</sub>	i-C <sub>3</sub> H <sub>7</sub>	1,2	65,40	32-3	10.80	9.60
C <sub>6</sub> H <sub>5</sub>	CH <sub>3</sub>	1	62	118	10.55	10.50
C <sub>6</sub> H <sub>5</sub>	C <sub>2</sub> H <sub>5</sub>	1	82	53	9.63	8.95
C <sub>6</sub> H <sub>5</sub>	n-C <sub>3</sub> H <sub>7</sub>	1	70	41	8.86	8.47 <sup>a</sup>
C <sub>6</sub> H <sub>5</sub>	i-C <sub>3</sub> H <sub>7</sub>	1	88	108	8.86	8.64 <sup>b</sup>
C <sub>6</sub> H <sub>5</sub>	n-C <sub>4</sub> H <sub>9</sub>	1	33	ca.29	8.22	7.46
C <sub>6</sub> H <sub>5</sub>	i-C <sub>4</sub> H <sub>9</sub>	3	66	82.5-83.5	<u>c</u>	
C <sub>6</sub> H <sub>5</sub>	C <sub>6</sub> H <sub>5</sub>	3	70	145.5-146.5	<u>d</u>	

a Anal. for sulfur: Calcd: 18.3; Found: 18.0%.

b Anal. for sulfur: Calcd: 18.3; Found: 18.0%.

c Anal. for carbon: Calcd: 44.50; Found: 44.74%. Anal. for hydrogen:  
Calcd: 6.15; Found: 6.33%.

d Anal. for carbon: Calcd: 51.75; Found: 51.52%. Anal. for hydrogen:  
Calcd: 3.63; Found: 3.49%.

Table II. Tin-119m Mössbauer Data for  $R_2Sn[S_2P(OR')_2]_2$  at 77K

<u>R</u>	<u>R</u>	<u>IS</u> <sup>a,b</sup>	<u>QS</u> <sup>a,c</sup>	<u>Γ</u> <sub>+</sub> <sup>a,c</sup>	<u>Γ</u> <sub>-</sub> <sup>a,c</sup>	<u>ρ</u> <sup>d</sup>
C <sub>6</sub> H <sub>5</sub>	CH <sub>3</sub>	1.35	3.34	1.07	1.47	2.47
C <sub>6</sub> H <sub>5</sub>	C <sub>2</sub> H <sub>5</sub>	1.41	3.12	1.07	1.20	2.21
C <sub>6</sub> H <sub>5</sub>	n-C <sub>3</sub> H <sub>7</sub>	1.42	3.22	1.11	1.16	2.27
C <sub>6</sub> H <sub>5</sub>	i-C <sub>3</sub> H <sub>7</sub>	1.40	3.67	1.14	1.24	2.62
C <sub>6</sub> H <sub>5</sub>	i-C <sub>4</sub> H <sub>9</sub>	1.43	3.62	1.15	1.28	2.53
C <sub>6</sub> H <sub>5</sub>	C <sub>6</sub> H <sub>5</sub>	1.47	3.21	1.40	1.80	2.18
CH <sub>3</sub>	CH <sub>3</sub>	1.43	3.35	1.09	1.30	2.34
CH <sub>3</sub>	C <sub>2</sub> H <sub>5</sub>	1.44	3.34	1.32	1.62	2.32

<sup>a</sup> In  $\text{mms}^{-1}$ .

<sup>b</sup>  $\pm 0.02 \text{ mms}^{-1}$ .

<sup>c</sup>  $\pm 0.05 \text{ mms}^{-1}$ .

<sup>d</sup>  $\rho = QS/IS$ .



Table III. Pmr Data for  $R_2Sn[s_2P(OR')_2]_2$ .<sup>a,b</sup>

<u>R</u>	<u>R'</u>	Chemical Shifts ( $\delta$ , ppm) and Coupling Constants (J, Hz)
CH <sub>3</sub>	CH <sub>3</sub>	3.70, d, 12H(OCH <sub>3</sub> ), $ ^3J(^{31}P-O-C-^1H)  = 15.5$ ; 1.52, s, 6H(Sn-CH <sub>3</sub> ); $ ^2J(^{119,117}Sn-C-^1H)  = 80.0$ , 76.
CH <sub>3</sub>	C <sub>2</sub> H <sub>5</sub>	4.12, dq, 8H(OCH <sub>2</sub> -), $ ^3J(^{31}P-O-C-^1H)  = 10.0$ , $ ^3J(^1H-C-C-^1H)  = 7.5$ ; 1.58, s, 6H(Sn-CH <sub>3</sub> ), $ ^3J(^{117,119}Sn-C-^1H)  = 79.0$ , 75.0; 1.38, t, 12H(CH <sub>3</sub> ), $ ^3J(^1H-C-C-^1H)  = 7.5$ .
C <sub>6</sub> H <sub>5</sub>	CH <sub>3</sub>	8.13-7.33, m, 10H(C <sub>6</sub> H <sub>5</sub> -Sn); 3.48, d, 6H(OCH <sub>3</sub> ), $ ^3J(^{31}P-O-C-^1H)  = 15.5$ .
C <sub>6</sub> H <sub>5</sub>	C <sub>2</sub> H <sub>5</sub>	8.17-7.36, m, 10H(C <sub>6</sub> H <sub>5</sub> -Sn); 3.89, dq, 8H(OCH <sub>2</sub> -), $ ^3J(^{31}P-O-C-^1H)  = 10.0$ , $ ^3J(^1H-C-C-^1H)  = 7.0$ ; 1.16, t, 12H(CH <sub>3</sub> ), $ ^3J(^1H-C-C-^1H)  = 7.0$ .
C <sub>6</sub> H <sub>5</sub>	n-C <sub>3</sub> H <sub>7</sub>	8.16-7.32, m, 10H(C <sub>6</sub> H <sub>5</sub> -Sn); 3.73, dt, 8H(OCH <sub>2</sub> -), $ ^3J(^{31}P-O-C-^1H)  = 9.5$ , $ ^3J(^1H-C-C-^1H)  = 6.5$ ; 1.77-1.23, m, 8H(-CH <sub>2</sub> -); 0.80, t, 12H(CH <sub>3</sub> ), $ ^3J(^1H-C-C-^1H)  = 7.0$ .
C <sub>6</sub> H <sub>5</sub>	1-C <sub>3</sub> H <sub>7</sub>	8.19-7.37, m, 10H(C <sub>6</sub> H <sub>5</sub> -Sn); 4.42, m, 4H(OCH-); 1.14, d, 24H(CH <sub>3</sub> ), $ ^3J(^1H-C-C-^1H)  = 6.0$ .
C <sub>6</sub> H <sub>5</sub>	1-C <sub>4</sub> H <sub>9</sub>	8.27-7.20, m, 10H(C <sub>6</sub> H <sub>5</sub> -Sn); 3.53, dd, 8H(OCH <sub>2</sub> -), $ ^3J(^{31}P-O-C-^1H)  = 9.0$ , $ ^3J(^1H-C-C-^1H)  = 7.5$ ; 1.73, m, 4H(-CH-); 0.82, d, 24H(CH <sub>3</sub> ), $ ^3J(^1H-C-C-^1H)  = 7.0$ .
C <sub>6</sub> H <sub>5</sub>	C <sub>6</sub> H <sub>5</sub>	7.83-6.80, m, 30H(C <sub>6</sub> H <sub>5</sub> -Sn, OC <sub>6</sub> H <sub>5</sub> ).

<sup>a</sup> In CDCl<sub>3</sub>; TMS as internal standard.

<sup>b</sup> s=singlet, d=doublet, t=triplet, m=multiplet, dd=doublet of doublets, dt=doublet of triplets, dq=doublet of quartets.

Table IV. Infrared Frequencies ( $\text{cm}^{-1}$ ) for  $\text{R}_2\text{Sn}[\text{S}_2\text{P}(\text{OR}')_2]_2$  in the Range 1400-2000  $\text{cm}^{-1}$ <sup>a,b</sup>

<u>R</u>	<u>R'</u>	
$\text{CH}_3$	$\text{CH}_3$	1300w, 1170s, 1025vs(vbr), 780vs(br), 650s(br), 550sh, 495sh, 485m, 365vvw, 350vvw, 300w, 275w, 255w, 215w.
$\text{CH}_3$	$\text{C}_2\text{H}_5$	1385m, 1283w, 1155m, 1090m, 1020sh, 1005vvs, 935vvs, 765vvs, 645s(br), 540sh, 505m, 375sh, 365sh, 355sh, 340-220w(br) showing slight fine structure.
$\text{C}_6\text{H}_5$	$\text{CH}_3$	1315w, 1305sh, 1165vs, 1155vs, 1075vs, 1035vvs, 1015vvs, 975sh, 793vs, 785sh, 725m, 690m, 653, 605sh, 587s, 535m, 490w, 440w(br).
$\text{C}_6\text{H}_5$	$\text{C}_2\text{H}_5$	1329w, 1295w, 1195vvw, 1153m, 1090w, 1040s(br), 1003vs, 947vs, 915sh, 810s, 797sh, 790s, 782sh, 722m, 685w, 635s(br), 500w, 470sh, 440w(br).
$\text{C}_6\text{H}_5$	$n\text{-C}_3\text{H}_7$	1335w, 1295w, 1250w, 1160sh, 1145w, 1125w, 1090sh, 1050vs, 1010sh, 985vvs(br), 960sh, 900s, 890m, 845vs, 830sh, 740sh, 725vs, 683s, 640vs(br), 600sh, 510m(br), 445w, 365vvw, 355vvw, 245w.
$\text{C}_6\text{H}_5$	$i\text{-C}_3\text{H}_7$	1342w, 1307w, 1260vvw, 1179m, 1145w, 1108w, 1002vs, 964vvs, 915w, 892m, 790m, 738w, 695w, 610mw, 520w, 440w.
$\text{C}_6\text{H}_5$	$i\text{-C}_4\text{H}_9$	1290w, 1270w, 1155vw(br), 1030sh, 1015sh, 990vs, 960sh, 904w, 850m, 820sh, 717w, 680w, 660w, 610w(br), 535w, 520sh, 440w, 410sh, 230vw.
$\text{C}_6\text{H}_5$	$\text{C}_6\text{H}_5$	1210w, 1187s, 1160s, 1070vw, 1022vw, 1000vw, 985s, 920vs, 900s, 783s, 770sh, 750w, 745sh, 728m, 688m, 665ms, 655ms, 570w(br), 515w(br), 420vvw.

<sup>a</sup> Recorded as Nujol mulls on KBr plates and polyethylene film.

<sup>b</sup> vvs=very very strong, vs=very strong, s=strong, m=medium, w=weak, vw=very weak, vvww=very very weak, sh=shoulder, br=broad.

Table V. Mass Spectral Data for  $R_2Sn[S_2P(OR')_2]_2$ .<sup>a</sup>

$R=CH_3$ ,  $R'=C_2H_5$

Mass Number	Rel. Abund.	Assignment
505	0.7	$CH_3Sn[S_2P(OC_2H_5)_2]_2^+$
490	0.7	$Sn[S_2P(OC_2H_5)_2]_2^{++}$
355	19.3	?
335	100.0	$(CH_3)_2SnS_2P(OC_2H_5)_2^+$
327	10.8	$355-C_2H_4^+$
307	22.0	$(CH_3)_2SnS_2P(OC_2H_5)OH^+$
305	24.2	$SnS_2P(OC_2H_5)_2^+$
299	13.2	$355-2C_2H_4^+$
279	26.4	$(CH_3)_2SnS_2P(OH)_2^+$
277	26.2	$SnS_2P(OC_2H_5)OH^+$
261	11.1	$(CH_3)_2SnS_2PO^+$
249	12.4	$SnS_2P(OH)_2^+$
247	10.7	$SnS_2PO_2^+$
245	13.9	$(CH_3)_2SnS_2P^+$
231	7.6	$SnS_2PO^+$
215	4.9	$SnS_2P^+$
183	12.1	$SnSP^+$
152	4.4	$SnS^+$
151	7.5	$SnP^+$
150	3.6	$(CH_3)_2Sn^{++}$
135	5.3	$(CH_3)Sn^+$
120	2.5	$Sn^{++}$

Table V. (continued)

$R=C_6H_5^-$   $R'=C_3H_7^-$

Mass Number	Rel. Abund.	Assignment
623	4.5	$C_6H_5Sn[S_2P(OC_3H_7)_2]_2^+$
546	0.5	$Sn[S_2P(OC_3H_7)_2]_2^{+*}$
487	67.7	$(C_6H_5)_2SnS_2P(OC_3H_7)_2^+$
445	26.5	$(C_6H_5)_2SnS_2P(OC_3H_7)(OH)^+$
403	55.6	$(C_6H_5)_2SnS_2P(OH)_2^+$
367	2.0	$(C_6H_5)SnS_2P(OC_3H_7)O^+$
359	6.3	?
333	7.4	$SnS_2P(OC_3H_7)_2^+$
325	30.5	$(C_6H_5)SnS_2P(OH)O^+$
307	7.9	$359-C_3H_6^+$
291	8.3	$SnS_2P(OC_3H_7)(OH)^+$
281	1.5	$359-C_6H_6^+$
261	6.3	$(C_6H_5)SnS_2^+$
249	16.3	$SnS_2P(OH)_2^+$
229	49.1	$(C_6H_5)SnS^{+*}$
197	11.9	$(C_6H_5)Sn^+$
183	1.6	$SnSP^{+*}$
120	5.0	$Sn^{+*}$

<sup>a</sup>Only tin-containing fragments are listed; mass numbers are based upon  $^{120}Sn$ ,  $^{32}S$ ,  $^{31}P$ ,  $^{16}O$ ,  $^{12}C$  and  $^1H$ .

Table VI. Tin-119m Mössbauer Quadrupole Splittings and the C-Sn-C Angles  
in Hexacoordinated Diphenyltin(IV) Compounds.

Compound	Q.S., $\text{mm s}^{-1}$	Ref.	$\angle\text{C-Sn-C}$ , deg.	Ref.
$(\text{C}_6\text{H}_5)_2\text{SnCl}_2 \cdot 2\text{DMSO}$ (1a) <sup>a</sup>	3.54	37	167.2(2), <sup>b</sup> 171.8(2) <sup>b,c</sup>	38
(1b) <sup>a</sup>	3.86	39		
$(\text{C}_6\text{H}_5)_2\text{SnCl}_2 \cdot \text{bipy}$ (2a) <sup>a</sup>	3.51	37	173.5(3) <sup>b</sup>	41
(2b) <sup>a</sup>	3.90	40		
$(\text{C}_6\text{H}_5)_2\text{Sn}[\text{S}_2\text{CN}(\text{C}_2\text{H}_5)_2]_2$ (3) <sup>a</sup>	1.74	42	101.4(6) <sup>b</sup>	43
$(\text{C}_6\text{H}_5)_2\text{Sn}[\text{S}_2\text{P}(\text{OC}_2\text{H}_5)_2]_2$ (4) <sup>a</sup>	3.12	<u>d</u>	135(1) <sup>b</sup>	13
$(\text{C}_6\text{H}_5)_2\text{Sn}[\text{S}_2\text{P}(\text{OC}_3\text{H}_7\text{-i})_2]_2$ (5) <sup>a</sup>	3.67	<u>d</u>	180.0(0) <sup>b</sup>	2
$(\text{C}_6\text{H}_5)_2\text{Sn}[\text{S}_2\text{P}(\text{OC}_6\text{H}_5)_2]_2$	3.21	<u>d</u>	142 <sup>e</sup>	
$(\text{C}_6\text{H}_5)_2\text{Sn}[\text{S}_2\text{P}(\text{OC}_3\text{H}_7\text{-n})_2]_2$	3.22	<u>d</u>	142 <sup>e</sup>	
$(\text{C}_6\text{H}_5)_2\text{Sn}[\text{S}_2\text{P}(\text{OCH}_3)_2]_2$	3.34	<u>d</u>	146.5 <sup>e</sup>	
$(\text{C}_6\text{H}_5)_2\text{Sn}[\text{S}_2\text{P}(\text{OC}_4\text{H}_9\text{-i})_2]_2$	3.62	<u>d</u>	159.5 <sup>e</sup>	

<sup>a</sup> Numbers in parentheses refer to Figure 1.

<sup>b</sup> Estimated standard deviations in parentheses.

<sup>c</sup> Mean values of these angles used in Figure 1.

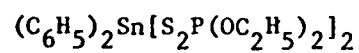
d This work.

<sup>e</sup> Values predicted using Equation 1.

Table VII. Low-Energy, Lattice-Mode Raman Frequencies and  $M_{\text{eff}}$  Values from the Effective Vibrating Mass Model.

<u>Compound</u>	<u><math>\omega</math></u>	<u><math>M_{\text{eff}}</math></u>	<u>Molecular Weight Multiple</u>
$(\text{C}_6\text{H}_5)_2\text{Sn}[\text{S}_2\text{P}(\text{OC}_2\text{H}_5)_2]_2$ (Mol. Wt. = 643.37)	28	680	1.06
	43	289	0.45
	58	159	0.25
$(\text{C}_6\text{H}_5)_2\text{Sn}[\text{S}_2\text{P}(\text{OC}_3\text{H}_7-1)_2]_2$ (Mol. Wt. = 699.49)	16	3793	5.42
	25	1546	2.21
	34	836	1.20
	63.5	240	0.34
	88	125	0.18

Table VIII. The Temperature Dependence of Mössbauer Spectral Areas for

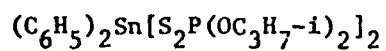


<u>T(K)</u>	<u>A<sub>+</sub><sup>a</sup></u>	<u>A<sub>-</sub><sup>a</sup></u>	<u>A<sub>TOTAL</sub>(T)</u>	<u>R=A+/A-</u>
77	0.078	0.088	0.167	0.898
85	0.066	0.074	0.140	0.892
95	0.053	0.061	0.114	0.869
105	0.044	0.051	0.095	0.863
115	0.035	0.045	0.080	0.778
125	0.028	0.035	0.063	0.800
135	0.023	0.028	0.051	0.821
145	0.015 <sup>b</sup>	0.028 <sup>b</sup>	0.043	0.536 <sup>b</sup>

a. A<sub>+</sub> and A<sub>-</sub> are the areas under the higher (more positive) and lower velocity components in the doublet spectrum, respectively.

b. These values are obviously erroneous and arise from inaccurate resolution of the total resonance into its components, A<sub>TOTAL</sub>(145) is, however, consistent with the other A<sub>TOTAL</sub>(T) data.

Table IX. The Temperature Dependence of the Mössbauer Spectral Areas for



<u>T(K)</u>	<u><math>A_+^a</math></u>	<u><math>A_-^a</math></u>	<u><math>A_{TOTAL}(T)</math></u>	<u><math>R=A+/A-</math></u>
77	0.061	0.062	0.123	0.984
85	0.054	0.058	0.112	0.931
95	0.047	0.053	0.100	0.887
105	0.043	0.049	0.092	0.878
115	0.039	0.043	0.082	0.907
125	0.036	0.041	0.077	0.878
135	0.031	0.038	0.069	0.816
145	0.027	0.031	0.058	0.871
155	$0.024^b$	$0.032^b$	0.056	$0.750^b$

a.  $A_+$  and  $A_-$  are the areas under the higher (more positive) and lower velocity components of the doublet spectrum, respectively.

b. These values are obviously erroneous and arise from inaccurate resolution of the total resonance into its components.  $A_{TOTAL}(155)$  is, however, consistent with all other  $A_{TOTAL}(T)$  data.



### Figure Captions

Figure 1. Correlation plot of tin-119m Mössbauer Quadropole Splittings (Q.S.) vs. the C-Sn-C angles in hexacoordinated diphenyltin(IV) derivatives.

Figure 2. The plot of  $\ln A$  (normalized to the area under the Mössbauer resonance curve at 77K) vs. temperature in K. The slopes are -1.92, -2.19 and  $-1.06 \times 10^{-2} \text{ K}^{-1}$  for the ethyl-, n-propyl- and i-propyl-derivatives.

Figure 3. The low-energy, lattice-mode Raman spectra of (a) bis-[0,0'-diethyl-dithiophosphatp]diphenyltin(IV) using a 488.0 nm laser source and (b) bis-[0,0'-diisopropyldithiophosphato]diphenyltin(IV) using a 476.5 nm laser source, both at 100 mw.

Figure 4. The temperature-dependence of  $\langle x_{II}^2 \rangle$  and  $\langle x_I^2 \rangle$  in  $\text{\AA}^2$  between 77 and 145K for bis-[0,0'-diethyldithiophosphato]diphenyltin(IV).

Figure 5. The temperature-dependence of  $\langle x_{II}^2 \rangle$  and  $\langle x_I^2 \rangle$  in  $\text{\AA}^2$  between 77 and 155K for bis-[0,0'-diisopropyldithiophosphato]diphenyltin(IV).

Fig 1.

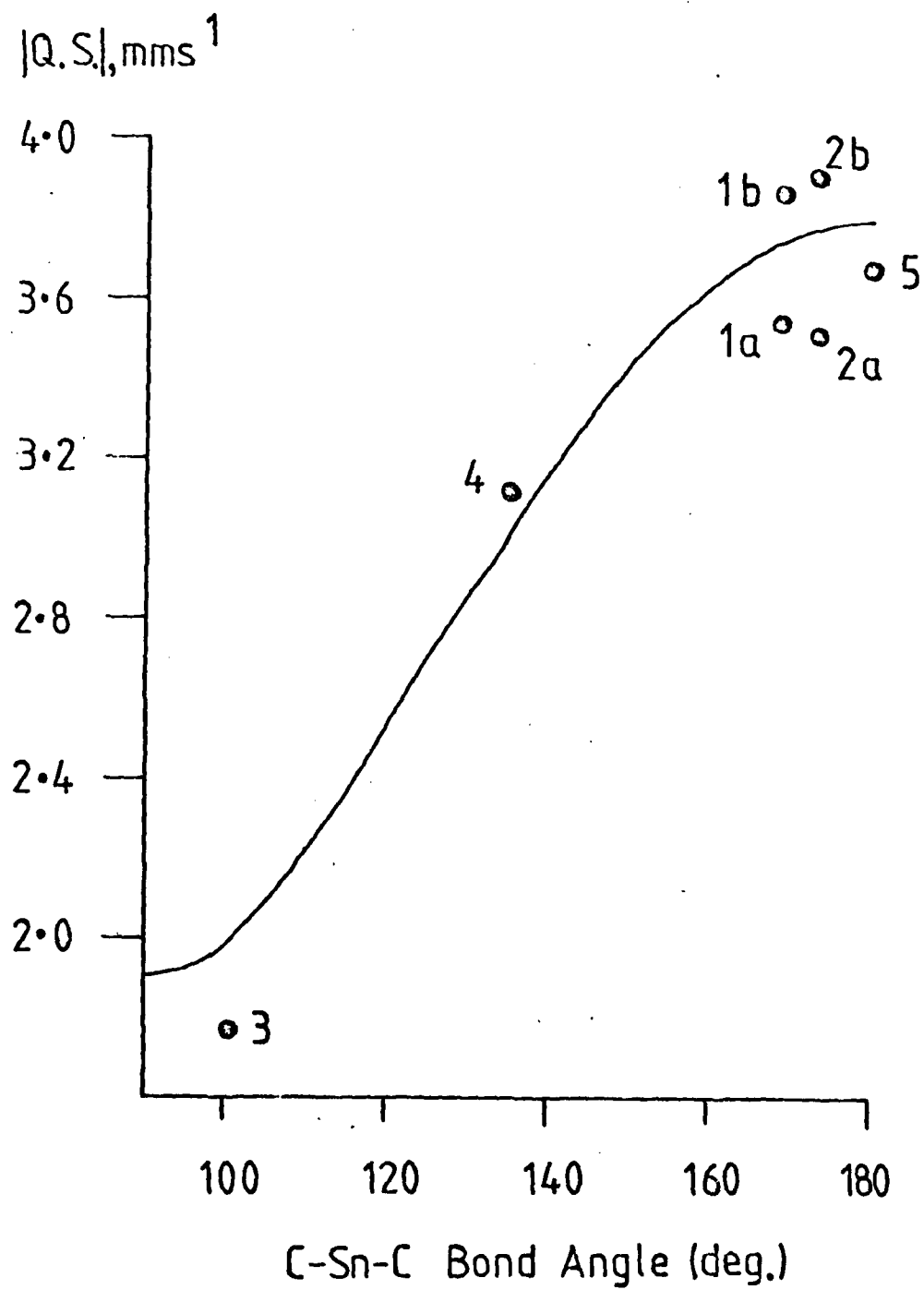


Fig 2.

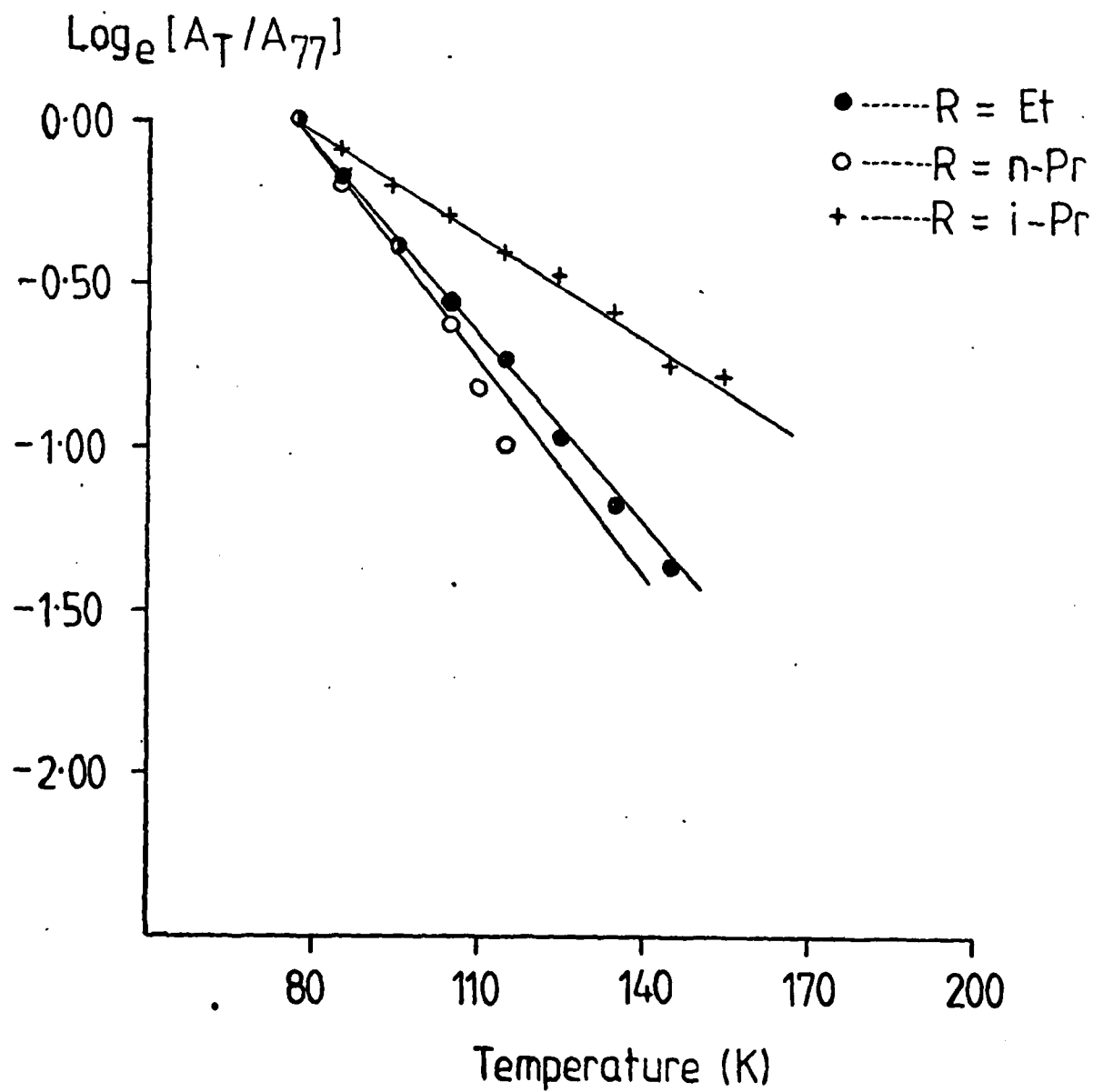
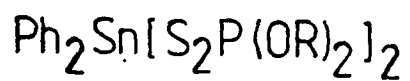


Fig 3

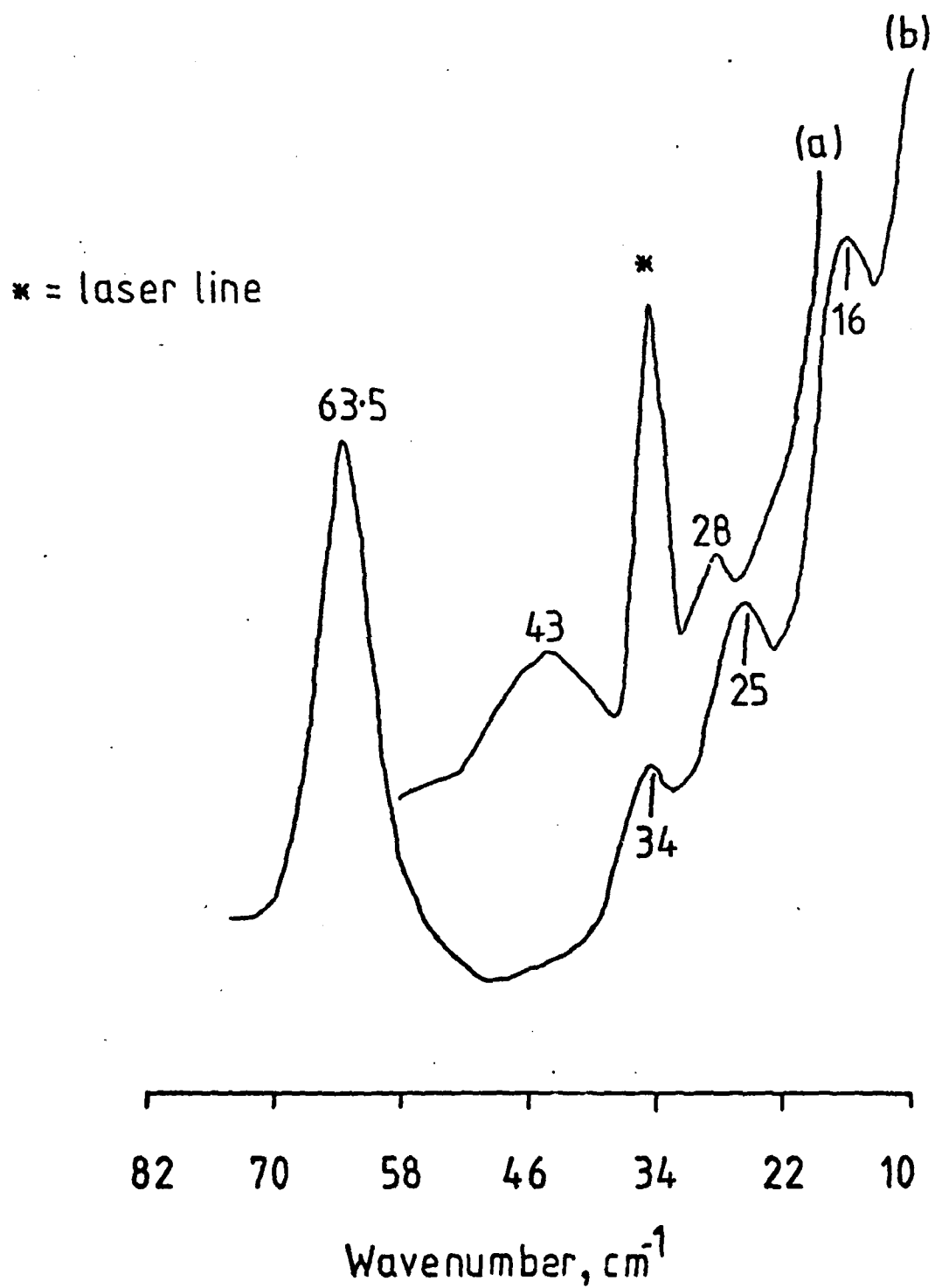


Fig 4

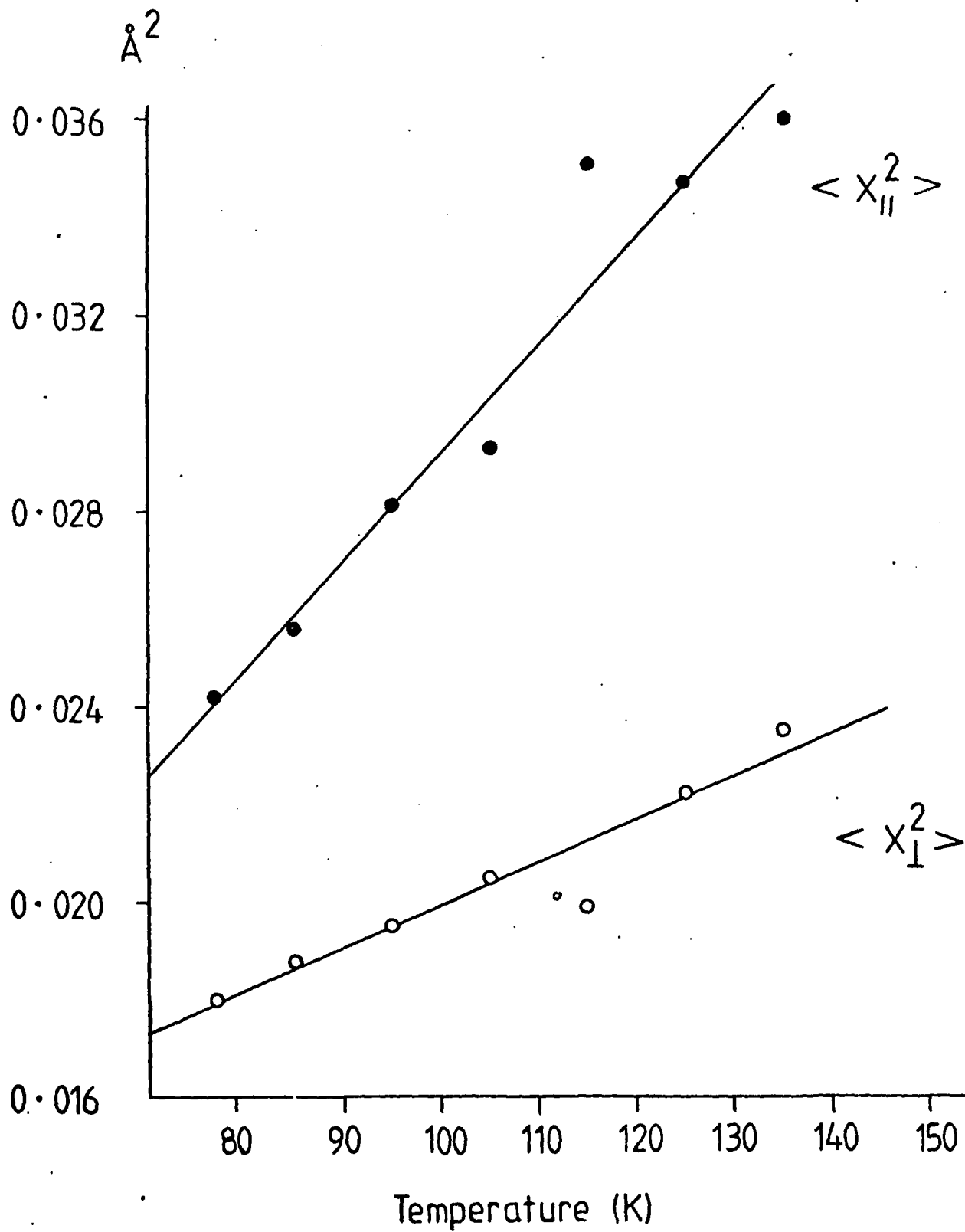
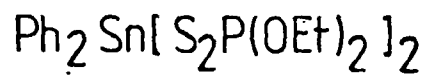


Fig 5

